Acta Materialia 155 (2018) 372–378

Contents lists available at ScienceDirect

Acta Materialia

journal homepage: www.elsevier.com/locate/actamat

Full length article

A new insight into the $\sum$=2 grain boundary characteristics in WC powder and in WC-Co sintered materials

Maxime Pellan [a, 1], Sabine Lay [a, *], Jean-Michel Missiaen [a], Susanne Norgren [b], Jenny Angseryd [b], Ernesto Coronel [c], Tomas Persson [d]

[a] Univ. Grenoble Alpes, CNRS, Grenoble INP, SIMAP, F-38000, Grenoble, France
[b] Sandvik Mining R&D Rock Tools, Stockholm, Sweden
[c] Sandvik Coromant R&D Stockholm, Sweden
[d] Seco Tools AB, Fagersta, Sweden

ARTICLE INFO

Article history:
Received 12 January 2018
Received in revised form
27 April 2018
Accepted 5 June 2018

Keywords:
WC-Co alloys
Grain boundaries
Sintering
Stacking faults
0-Lattice
Elastic energy of dislocations

ABSTRACT

In order to gain a better understanding of the WC-Co sintering process, the change in $\sum = 2$ grain boundaries was studied in two series of alloys with different carbon contents and increasing Co content in the 10–50 vol% range. The samples were sintered at 1410 °C for 1 h and 5 h. The frequency of $\sum = 2$ grain boundaries and the rotation angle distribution were determined using electron backscatter diffraction (EBSD) in order to make a statistical analysis of the effect of composition and sintering time on the special boundary characteristics. Complementary TEM observations were conducted for a more thorough determination of the rotation aspects (angle/axis). The rotation angle is scattered in the WC powder with a maximum peak close to 90°, as expected for $\sum = 2$ grain boundaries. However, the average rotation angle tends towards 88.7° in sintered alloys. This deviation is explained by a dislocation array compensating for the misfit and angular deviation in the grain boundary. Its characteristics are calculated using the 0-lattice approach and the associated elastic energy is evaluated from these data. The observed angular deviation is consistent with a minimum elastic energy of the boundary. Particle rearrangement, which can occur during liquid phase sintering, might explain the slight rotation of adjacent crystals in the sintered materials, in order to find a lower energy configuration. A mechanism involving stacking faults in successive prismatic planes is also proposed to explain the formation of $\sum = 2$ boundaries and their high frequency in the powder.

1. Introduction

WC-Co cemented carbides are used for a large panel of applications such as cutting or drilling tools and their mechanical properties are tailored by adjusting the WC grain size and Co content. The material is prepared by the powder metallurgy route. Liquid phase sintering occurs with a cobalt rich liquid acting as a binder for the WC phase after solidification. The fraction of WC grain boundaries diminishes as the binder content increases [1,2], and specific boundary planes are identified [3–5]. The WC powder used for the fabrication of WC-Co alloys is polycrystalline most of the time [6], and special boundaries are found to be present both in the WC powder and in the sintered material [7,8]. Among these grain boundaries, so called $\sum = 2$ grain boundaries and especially $\sum = 2$ twist boundaries are predominant. The presence of such boundaries, first identified by TEM in the sintered alloys [9,10], was further confirmed by EBSD studies [3,11]. The grain boundary resistance upon cobalt infiltration during sintering was estimated for several grain boundary orientations using ab-initio calculations and it was deduced that $\sum = 2$ grain boundaries present in the powder were stable [12]. A large number of such grain boundaries in the cemented carbide probably arise from the powder while most other boundaries form during sintering due to impingement of the WC grains. Small rotations of WC grains are also expected to occur during sintering, in order to lower the overall grain boundary energy [5].

A precise knowledge of the grain boundary population characteristics in the WC powder and after sintering is necessary for a

* Corresponding author. SIMAP, Domaine Universitaire, 1130, rue de la piscine, BP 75, 38402, Saint Martin d'Hères, France.
E-mail address: sabine.lay@simap.grenoble-inp.fr (S. Lay).
[1] Present address, Sandvik Hyperion SAS, Grenoble, France.

https://doi.org/10.1016/j.actamat.2018.06.022
1359-6454/

better knowledge of the sintering mechanisms and for a better control of the material microstructure and properties. This work focuses on $\sum = 2$ boundaries found in the powder and in the sintered carbide and especially on the change in the orientation relationship as a function of cobalt content. A deviation from the 90° twist rotation angle of $\sum = 2$ boundaries is noted in sintered materials. The results are interpreted using the 0-lattice theory by calculating the density and orientation of misfit dislocations lying in the boundary plane as a function of the misorientation [13]. The grain boundary elastic energy is evaluated for the calculated dislocation array and equilibrium rotation angles are deduced and compared to the experiments. The mechanisms of $\sum = 2$ grain boundary formation in the powder and their stability during sintering are then reviewed from the results.

2. Experimental procedure

WC-Co alloys were sintered at 1410 °C for 1 and 5 h with 10, 15, 20, 30, 40 and 50 vol % Co. C-rich and W-rich compositions were chosen in the two phase domain at the limit with the three phase domains at 1000 °C. WC powder from HC Stark with a mean grain size of 0.6 μm was used. In order to analyze grain boundaries in the WC powder, organic compounds and cobalt were removed from a powder mixture after milling and WC powder was consolidated by sintering with 40 wt% Cu at 1120 °C for 15 min under He/H2 atmosphere. Solubility in Cu is sufficiently low at this temperature to consider that WC powder is unchanged by the preparation.

All samples were mechanically polished down to 1/10 μm, then Ar-milled using a Gatan Precision Ion Polishing System for 2 h with a 2° incident angle and a 2 kV accelerating voltage for EBSD characterization. EBSD experiments were carried out using a Zeiss Supra 55 VP microscope with a field ion gun, equipped with the EBSD HKL NordlysMax detector and the data were processed using Channel 5 Suite AZtec software. Five 30×30 μm maps were collected for each sample with a step size of 40 nm and an accelerating voltage of 20 kV. The hexagonal WC, cubic and hexagonal Co phases were identified from the patterns. Most non-indexed points are located at phase boundaries or in Co. A cleaning operation using the Channel 5 suite software was performed. Grain mapping was obtained using a minimum misorientation for grain boundaries of 2° and a minimum grain size of six pixels (0.1 μm), much smaller than the mean grain size of WC grains after sintering (1–2 μm). The Aphelion™ image analysis software was used to extract orientation information from the EBSD maps. WC boundary misorientations were determined by a dedicated Matlab™ program [5,14].

Among the twelve equivalent descriptions for a hexagonal structure, the angle/axis pair associated with the smallest angle was chosen. According to experimental conditions, the angular resolution on the misorientation angle at a grain boundary in EBSD is considered to be close to 0.5° [15]. Moreover, a tolerance angle of 5° on the orientation of the rotation axis was used to analyse the boundary population in the alloys. Complementary transmission electron microscopy (TEM) observations were conducted using a JEOL 3010 microscope running at 300 kV. TEM thin foils were prepared by mechanical polishing and ion beam milling.

3. Results

The most frequent rotation axis is $[10\bar{1}0]$ [5], representing about 25% of the boundary surface in the powder and 10%–20% in sintered materials as the Co fraction increases from 10 to 50 vol.% (Fig. 1a). The value for 50 vol.% Co is close to the powder value. The distribution of rotation angles around the $[10\bar{1}0]$ axis was determined for the powder and for the sintered materials (Fig. 1b). The

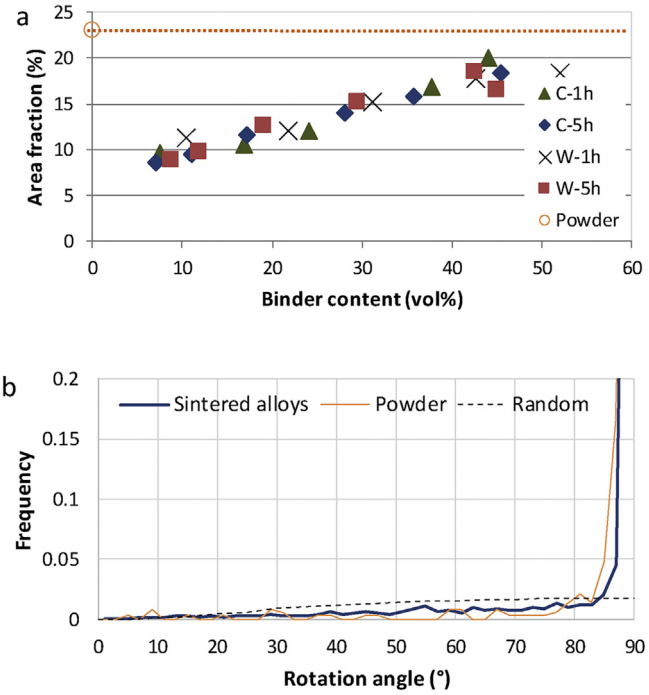

Fig. 1. (a) Fraction of boundaries corresponding to the $[10\bar{1}0]$ rotation axis in C-rich and W-rich alloys sintered for 1 h and 5 h, and for the powder. (b) Distribution of rotation angles measured for the $[10\bar{1}0]$ rotation axis in sintered alloys and in the powder. The random distribution of rotation angles for a hexagonal material is also drawn [16].

angle distribution shows a sharp peak around 90° for all alloys and for the powder, compared with a random distribution for a hexagonal material [16]. This peak corresponds to grain boundaries labelled $\sum = 2$ using the coincident site lattice framework (CSL) and approximating the c/a lattice parametric ratio of WC (=0.97) by 1 [9]. In this approach, the $\sum = 2$ boundary is described by a rotation of 90° around the $[10\bar{1}0]$ axis (Fig. 2).

3.1. Rotation angle distribution of $\sum = 2$ grain boundaries

EBSD data provide some indications on the rotation angle of $\sum = 2$ boundaries in the powder and in the sintered materials. Between 100 and 400 grain boundaries were found with a rotation axis of $[10\bar{1}0]$ and an angle in the [85°–90°] range for each sample. No influence of the carbon content or sintering time on the rotation angle distribution is detected. A wider distribution of rotation angles is observed in the powder compared to the sintered alloys (Fig. 3). The maximum peak value is close to 88.7° in the sintered alloys.

Accurate measurements of orientation relationships for $\sum = 2$ boundaries were also conducted by TEM in a sintered alloy using a method based on the Kikuchi line position [17]. For all the grain boundaries studied, the boundary plane was found to be parallel to the $(10\bar{1}0)$ plane perpendicular to the $[10\bar{1}0]$ rotation axis. The $\left[\bar{1}2\bar{1}0\right]$ direction of one grain was positioned parallel to the electron beam. For a misorientation angle of 90°, this direction should be exactly parallel to the [0001] direction of the second grain (Fig. 2c). Any twist deviation causes a shift in the Kikuchi lines parallel to the boundary plane while a tilt deviation causes a shift perpendicular to the boundary plane (Fig. 4). The shift vector between the $\left[\bar{1}2\bar{1}0\right]$ and [0001] zone axes was determined for several